Journal of Power Sources 271 (2014) 556–560

Contents lists available at ScienceDirect

Journal of Power Sources

journal homepage: www.elsevier.com/locate/jpowsour

Short communication

Operando studies of all-vanadium flow batteries: Easy-to-make reference electrode based on silver–silver sulfate

Edgar Ventosa [a, *], Marcel Skoumal [a], Francisco Javier Vázquez [a], Cristina Flox [a], Joan Ramon Morante [a, b]

[a] Catalonia Institute for Energy Research, Jardins de les Dones de Negre, e1, 08930 Sant Adria de Besos, Barcelona, Spain
[b] Departament d'Electronica, Facultat deFisica, Universitat de Barcelona, Martí i Franques 1, 08028 Barcelona, Spain

HIGHLIGHTS

- Studies of all-vanadium flow batteries are carried out in operando conditions.
- The construction of a reliable and easy-to-make reference electrode is described.
- Ammoxidized graphite felts are evaluated.
- The kinetic of the redox reactions is slower at positive electrode.

GRAPHICAL ABSTRACT

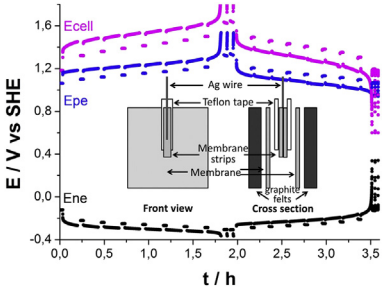

ARTICLE INFO

Article history:
Received 7 July 2014
Received in revised form
21 July 2014
Accepted 7 August 2014
Available online 15 August 2014

Keywords:
Vanadium redox flow batteries
Reference electrode
Operando conditions
Electrode kinetics
Ammoxidized graphite felts

ABSTRACT

In-depth evaluation of the electrochemical performance of all-vanadium redox flow batteries (VRFBs) under operando conditions requires the insertion of a reliable reference electrode in the battery cell. In this work, an easy-to-make reference electrode based on silver–silver sulfate is proposed and described for VRFBs. The relevance and feasibility of the information obtained by inserting the reference electrode is illustrated with the study of ammoxidized graphite felts. In this case, we show that the kinetic of the electrochemical reaction VO^{2+}/VO_2^+ is slower than that of V^{2+}/V^{3+} at the electrode. While the slow kinetics at the positive electrode limits the voltage efficiency, the operating potential of the negative electrode, which is outside the stability widow of water, reduces the coulombic efficiency due to the hydrogen evolution.

1. Introduction

The management of electrical grid performances and the integration of renewable energy sources with intermittent energy production require the deployment of large-scale energy storage. Redox flow batteries are promising candidates for grid-energy storage due to the long life, low cost, high round-trip efficiency and independent scalability of energy and power capabilities [1–4]. Among all redox flow battery technologies, all-vanadium redox flow batteries (VRFBs) are the most studied and mature. The main advantage of VRFBs is to use the same element, vanadium, as active material for both the positive electrolyte, VO^{2+}/VO_2^+, and the negative electrolyte, V^{2+}/V^{3+}. Nevertheless, VRFBs require a decrease in the costs for further advance into the market. One way of achieving it is to increase the energy efficiency and the power capability. The former will allow storing reversibly more energy at

* Corresponding author.
E-mail address: eventosa@irec.cat (E. Ventosa).

http://dx.doi.org/10.1016/j.jpowsour.2014.08.029
0378-7753/

the same cost, while the latter will allow limiting the size of the stack and, thus, reducing the cost [5].

One approach for improving the energy efficiency and power capability is to enhance the performance of the electrode materials. For instance, introducing oxygenated and/or nitrogenated groups [6–9] onto carbonaceous felts as well as modifications with Bi [10], Mn_3O_4 [11] or WO_3 [12] have shown improved performance of the battery. In-depth electrochemical evaluation of the electrodes under operando conditions is not trivial as it requires the insertion of a reference electrode into the filter press cell. The most widespread strategy is to characterize the electrodes by ex-situ methods in a bulky three-electrode cell prior to the full cell tests. Recently, Zawodzinski's group has shown interesting results for carbon paper electrodes by inserting a dynamic hydrogen reference electrode in a filter press cell [13–15].

Here we present a reliable and easy-to-make reference electrode for the evaluation of VRFBs in operando condition. We illustrate the valuable information obtained by using this reference electrode with the exemplary case of the evaluation of the electrochemical properties of ammoxidized graphite felts, which contains both oxygenated and nitrogenated groups.

2. Experimental section

A home-made filter press cell was used (Fig. 1a). Briefly explained, two pieces of porous carbon material (graphite felt) acting as positive and negative electrodes are pressed against each other by two bipolar plates. An ion exchange membrane is placed between the electrodes and the vanadium containing electrolytes are forced to flow through the carbon felts. The system is sealed using gaskets to avoid leakage of electrolyte. Silver wire of 0.5 mm diameter was purchased from Sigma–Aldrich. Ammoxidized graphite felt (RVG 2000 from Mersen) and anionic-exchange membrane (Fumasep FAP-450 from Fumatech) were used as electrode and separator, respectively. Graphite felt was ammoxidized by annealing the pristine material at 500 °C for 24 h under NH_3/O_2 atmosphere (1:1) [7]. The electrolytes were prepared electrochemically from a solution of 1 M $VOSO_4$ (Alfa Aesar) in 3 M H_2SO_4 (Sigma–Aldrich). All electrochemical measurements were carried out using a Biologic VMP-3 potentiostat at 21 ± 2 °C.

3. Results and discussion

The reference electrode consisted of a silver wire, two pieces of ion-exchange membrane and two pieces of Teflon tape (Fig. 1b). The silver wire was sandwiched between two rectangular pieces of membrane. Some drops of 3 M sulfuric acid were added to ensure good wettability. The stack formed by membrane/Ag wire/membrane was again sandwiched between two pieces of Teflon tape. Teflon is highly hydrophobic and, thus, it acted as physical barrier and maintained our reference electrode separated from the solution. The bottom of the membrane was not covered by the Teflon to allow ionic contact between the Ag wire and the solution. In absence of the membrane pieces, the Ag wire remains ionically insulated from the solution. The Teflon pieces are employed to prevent any possible diffusion of Ag_2SO_4 through the thin membrane (50 μm of thickness). The reference electrode composed of Teflon/membrane/Ag wire/membrane/Teflon was inserted between the two membranes that separate the positive and negative electrodes. The rest of the cell was assembled as any filter press VRFB [16] (Fig. 1a). The silver wire was slightly oxidized to obtain a thin layer of silver sulfate by applying 1 mA for 1 min in the assembled cell.

Fig. 2 shows the potential profiles of several charge − discharge cycles at 20 mA cm^{-2} and 30 mL min^{-1}. The use of the reference electrode allowed the potential profiles of positive and negative electrode to be monitored separately. The limiting side (positive or negative) can be easily identified, enabling facile balancing of the two electrolytes. In this case, both electrolytes seemed quite balanced. The positive electrode forced the end of the charge while the negative electrode was responsible for the end of the discharge (except for the first cycle). This means that an irreversible reaction (hydrogen evolution) occurred simultaneously to the reduction of V^{3+} at the negative electrode during the charge. As a result, V^{+3} was not entirely reduced to V^{2+}, whereas VO^{2+} was completely oxidized to VO_2^+ forcing the end of the charge. During the discharge, there was not enough V^{2+} to balance VO_2^+. Fig. 2 also reveals that the

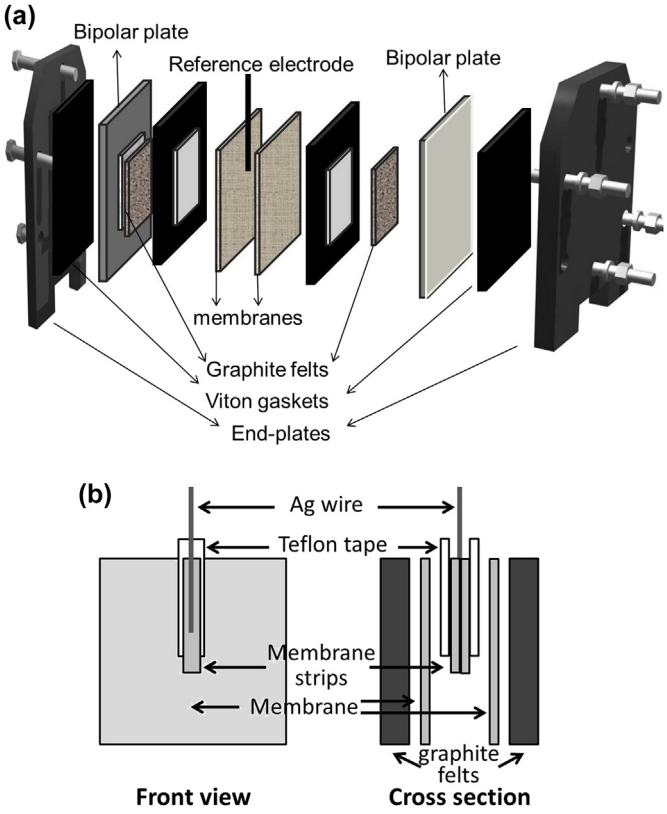

Fig. 1. Scheme of (a) a filter press cell and (b) the proposed reference electrode.

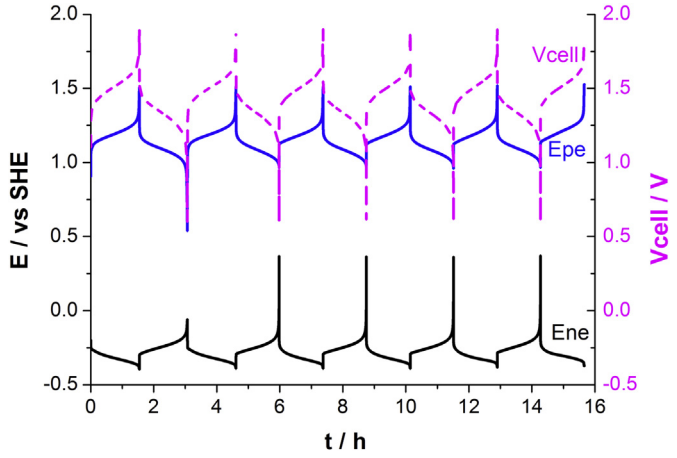

Fig. 2. Potential profile of VRFB upon cycling at 20 mA cm^{-2} and 30 mL min^{-1}.

potential of our reference electrode was stable under operating conditions.

The potential of the electrodes is given by the Nernst equation (Eq. (1)), where E^0 is the standard potential, R is the gas constant, T is the temperature, n is the number of involved electrons, F is the Faraday constant and a_{red} and a_{oxi} are the activities of the reduced and oxidized species, respectively.

$$E = E^0 - \frac{RT}{nF}\ln\frac{a_{red}}{a_{oxi}} \quad (1)$$

The redox reaction of the couple VO_2^+/VO^{2+} and V^{3+}/V^{2+} are described in Eqs (2) and (3), respectively.

$$VO_2^+ + 2H^+ + 1e^- \rightarrow VO^{2+} + H_2O \quad E^0 = 1.0\ \text{V vs SHE} \quad (2)$$

$$V^{3+} + 1e^- \rightarrow V^{2+} \quad E^0 = -0.26\ \text{V vs SHE} \quad (3)$$

The potential, versus standard hydrogen electrode (SHE), at the negative and positive electrode are given by the Eqs. (4) and (5), respectively. Eqs. (4) and (5) shows that the potential at the positive electrode (VO_2^+/VO^{2+}) depends on the activity of protons, while the potential at the negative electrode only depend on the activities of vanadium species.

$$E = -0.26 - 0.059\log\frac{a_{V^{2+}}}{a_{V^{3+}}} \quad (4)$$

$$E = 1.0 - 0.059\log\frac{a_{VO^{2+}}}{a_{VO_2^+}} + 0.118\log a_{H^+} \quad (5)$$

At 50% of state of charge (SoC), the potential at the negative electrode is −0.26 V vs SHE, whereas the potential at the positive electrode is pH-dependent as mentioned. Therefore, the potential of the reference electrode can be determined at open circuit at 50% of state of charge (SoC). The observed value of V^{3+}/V^{2+} of −0.625 V (versus our reference electrode) should be equal to −0.26 V (versus SHE). Inserting these values in Eq. (6), we obtained Eqs. (7) and (8). Thus, the potential of our reference electrode was +0.365 V versus SHE. Note that we represent all potential versus SHE for easy comparison with other studies. The advantage of a reference electrode inserted in an all-vanadium flow battery is that the potential of the couple at the negative electrode, V^{3+}/V^{2+}, at 50% SoC can be employed as standard for the internal calibration of the reference potential. For every new reference electrode, its potential can be determined following the above described methodology, i.e. the potential of the reference electrode can be calibrated and corrected in-situ. The observed potential of the positive electrode of 1.15 V (vs SHE) was slightly higher than expected due to effects of side processes such as water evaporation or oxygen evolution.

$$E_{ne} = E^0_{V^{2+}/V^{3+}} \quad \text{at 50\% SoC} \quad (6)$$

$$E_{ref} - 0.625 = E^0_{H_2/H^+} - 0.26 \quad (7)$$

$$E_{ref} = E^0_{H_2/H^+} + 0.365 \quad (8)$$

We further explored the stability of the reference electrode by monitoring the open circuit potential of an all-vanadium redox flow battery at 100% SoC. The voltage profile of the battery ($E_{positive} - E_{negative}$) decreased slightly over time due to the self-discharge of the cell (Fig. 3a), which was obvious by the change in color of the electrolytes. The individual potential of the positive and negative electrode (Fig. 3b) revealed that the potential of the two electrodes evolved in opposite direction; the positive electrode potential slowly decreased while the negative one increased. An overlapped sinusoidal oscillation of potential was observed when magnifying the potential profile of the electrode (Fig. 3c). That oscillation was the noise of the reference electrode because it occurred simultaneously in both electrodes. Therefore, the noise of the potential of the reference is ±10 mV within an interval of *ca.*

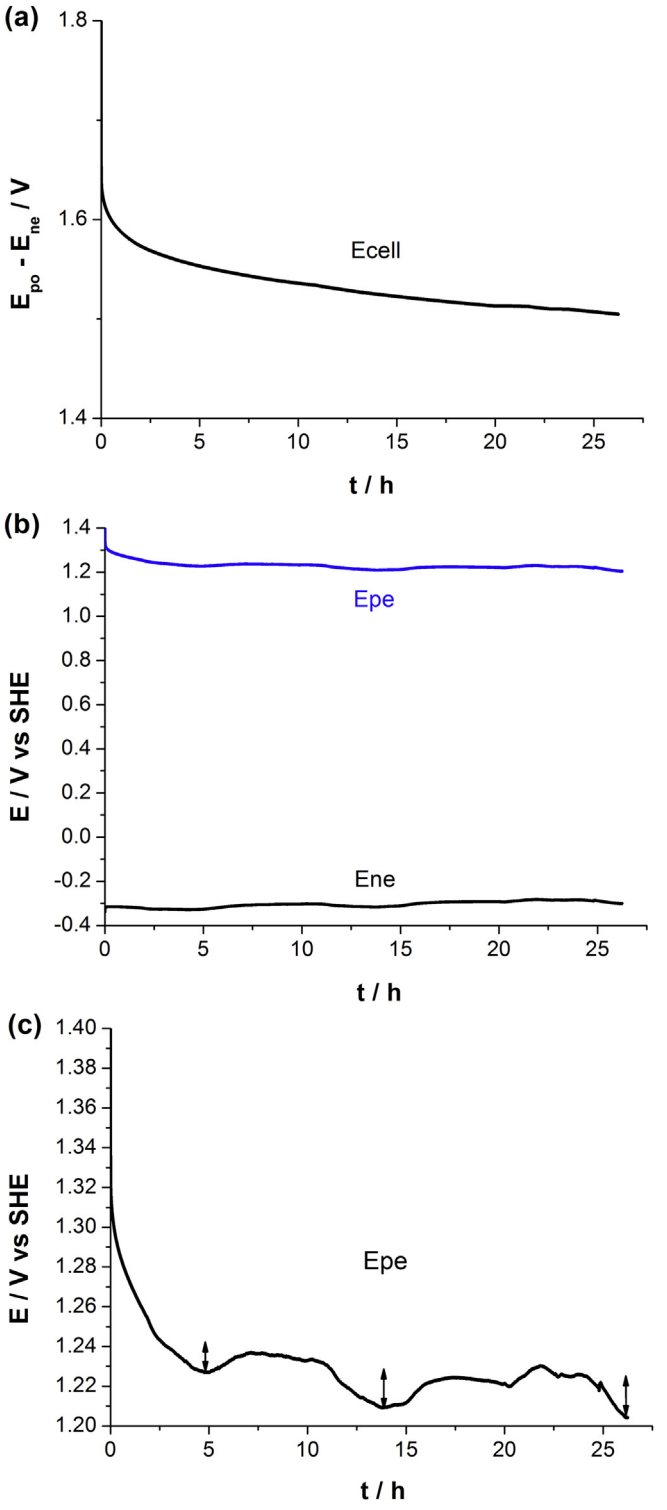

Fig. 3. Open circuit potential (OPC) at 100% SoC of (a) the battery, (b) the positive and negative electrode and (c) the magnification of the positive electrode.

10 h. Because of the low frequency of the noise (10 h), we consider this level of noise to be acceptable for this application, bearing always in mind this limitation when comparing potentials obtained with 10 h difference.

The ionic resistance of the electrolyte between reference electrode and graphite felt was determined by electrochemical impedance spectroscopy. Fig. 4 shows the Nyquist plot obtained for the positive (dashed black line) and the negative electrode (solid red line) (in web version). The ionic resistance is given by the Y-interception (imaginary part = 0). A value of 0.05 and 0.04 Ohm were obtained for the positive and negative electrode, respectively. The small values of ionic resistance are due to the large geometrical area of the electrode (25 cm^2). We used these ionic resistance values to correct the current intensity in the follow-up experiments.

We evaluated the kinetics of the electrochemical reactions at the positive and negative electrode of VRFB in operando conditions to illustrate the usefulness of our reference electrode. Fig. 5a shows the voltage profiles of the cell and potential profiles the positive and the negative electrode at several current densities in a galvanostatic measurement at around 50% SoC. The increase in potential with increased current is due to several factors; ionic resistance of the electrolyte, concentration overpotential and electrode kinetics overpotential. We corrected the ionic resistance of the electrolyte with the values obtained by EIS. We also used a flow as high as 70 mL min^{-1} to minimize the concentration gradients (second factor). Thus, the higher potential for higher current density (Fig. 5b) is significantly affected by the kinetic factor in this case. The potential incremented with increasing current step and it was always larger at the positive electrode. In addition, the increase in the potential increased with current step more rapidly at the positive electrode (Fig. 5c). The difference in the increment of potential between the positive and negative electrode stabilized above 64 mA cm^{-2} indicating that the concentration overpotential dominates at those current densities at 70 mL min^{-1}. The values obtained during the charge were always lower which was likely due to the evolution of hydrogen and oxygen.

Another example of electrochemical evaluation is shown in Fig. 6. Using galvanostatic intermittent titration technique (GITT), the thermodynamic potentials of the positive and negative electrode can be obtained. GITT consists in a galvanostatic charge – discharge measurement during which open circuit is periodically applied. The potential recorded during the open circuit periods exclude the contribution of the ionic resistance and the concentration overpotential as well as electron transfer resistance. In addition, GITT provides values of overpotentials under operando conditions, which are represented by double arrows in Fig. 3a. This information is very valuable, for example, to fit the theoretical calculation or to determine the overpotentials in the positive and negative electrode at different SoC. For ammoxidized graphite felts,

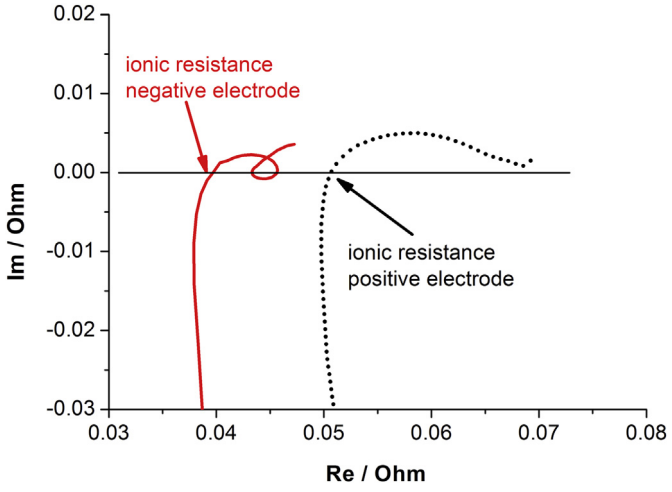

Fig. 4. EIS Nyquist plots of the positive (dashed black line) and negative electrode (solid red line) obtained at 50% of SoC. The frequency range was from 100 KHz to 0.1 Hz. (For interpretation of the references to colour in this figure legend, the reader is referred to the web version of this article.)

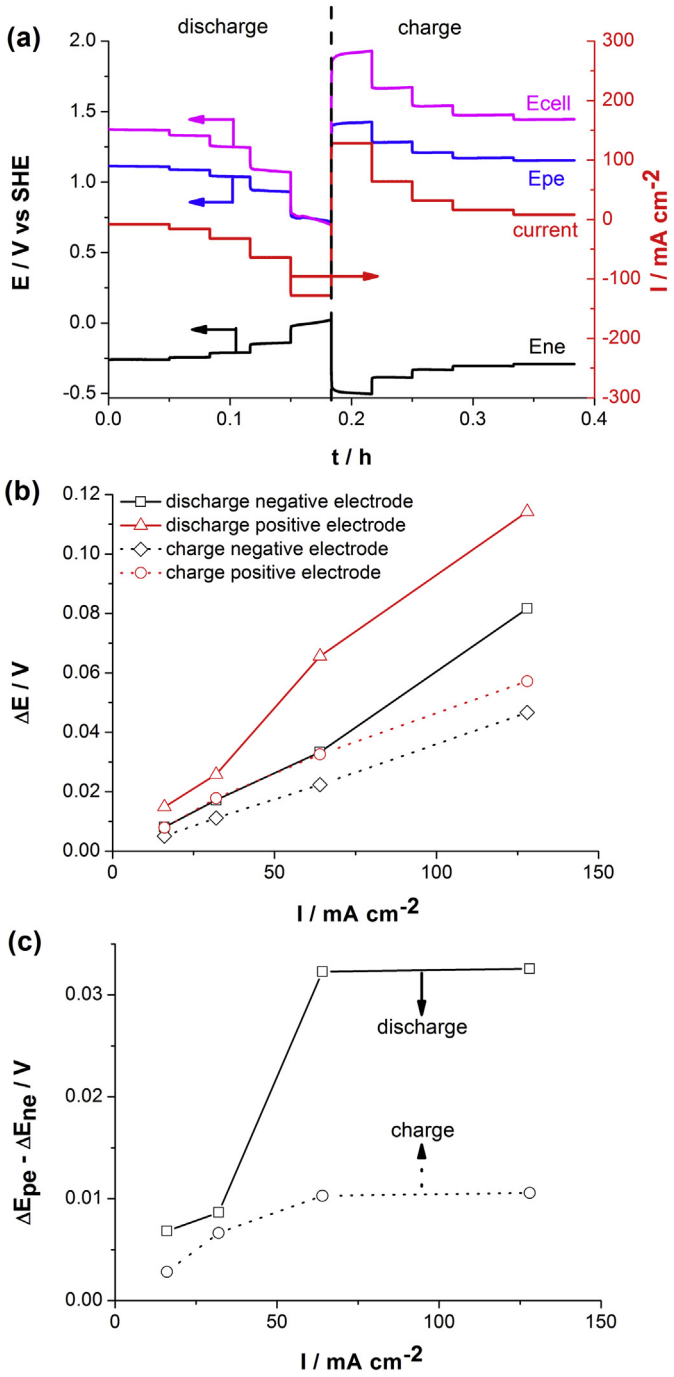

Fig. 5. (a) Potential profile of VRFB at different current densities (8, 16, 32, 64 and 128 mA cm^{-2}), (b) iR corrected potential increase observed for each step of current density and (c) differences between the potential increase of the positive and negative electrode for each current step. SoC and flow were around 50% and 70 mL min^{-1}, respectively.

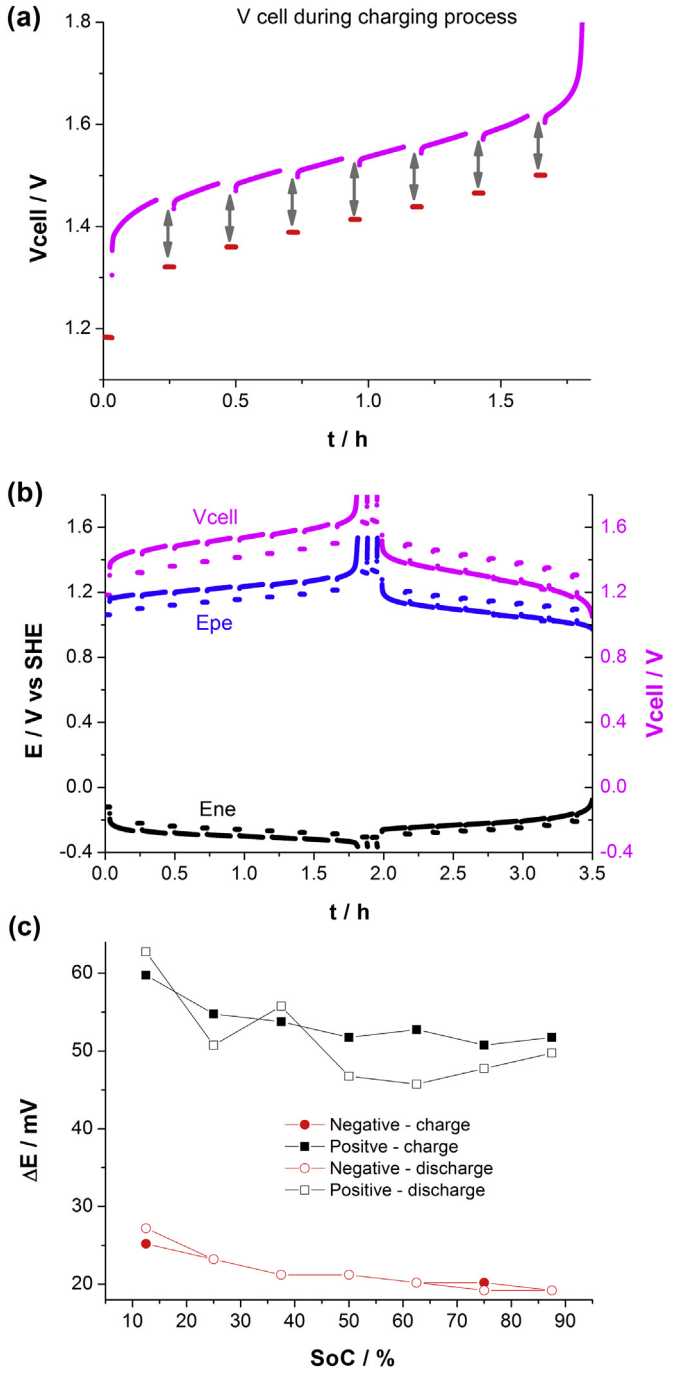

Fig. 6. (a) Voltage profile of the battery ($E_{positive} - E_{negative}$) during charging. (b) Voltage profiles of the battery ($E_{positive} - E_{negative}$) and potential profile of the positive electrode and negative electrode during charging and discharging. (c) Overpotentials at different states of charge. Galvanostatic intermittent titration technique (GITT) was carried out at 20 mA cm^{-2} and 70 mL min^{-1}.

the overpotentials during the discharge, in which the gas-evolution is absent, were slightly higher for low SoC (Fig. 3c), confirming the theoretical estimations [17]. You et al. calculated that the overpotentials increase sharply at very low and high SoC [17]. In our case, we also observed higher overpotentials at low SoC, although slightly lower values than the simulated ones likely due to the high flow rate used in our study. This fact indicates that there is a small contribution of the concentration on the overpotential at low SoC, even at 70 mL min^{-1} at 20 mA cm^{-2}. We did not observe an increase in overpotential at 87.5% SoC as theoretically predicted by You et al. [17]. The most likely explanation is that the actual SoC was slightly lower than the expected one due to the fast charging rate. More importantly, the overpotentials in the positive side were always significantly higher than those in the negative one, confirming the observations in the previous experiments, i.e. the slower kinetics at the positive electrode.

4. Conclusions

We have proposed a reference electrode based on silver–silver sulfate to be inserted in filter press cells of VRFB. This easy-to-make reference electrode provides valuable information for in-operando conditions. For ammoxidized graphite felts, the hydrogen evolution at the negative electrode during the charge decreases the coulombic efficiency whereas the slower kinetics of the positive electrode contributes more to the decrease in voltage efficiency. The use of this easy-to-make reference electrode also opens new perspectives for the experimental routes allowing a fast, reliable and feasible way for proceeding in the study, analysis and control of VRFBs.

Acknowledgments

This research was supported by the European Regional Development Funds (ERDF-FEDER Programa Competitivitat de Catalunya 2007–2013) and by the Ministerio de Economía y Competitividad-INNPACTO, project REDOX 2015 (IPT-2011-1690- 920000)

References

[1] Z.G. Yang, J.L. Zhang, M.C.W. Kintner-Meyer, X.C. Lu, D.W. Choi, J.P. Lemmon, J. Liu, Chem. Rev. 111 (2011) 3577.
[2] C.P. de Leon, A. Frias-Ferrer, J. Gonzalez-Garcia, D. Szanto, F.C. Walsh, J. Power Sources 160 (2006) 716.
[3] L. Joerissen, J. Garche, C. Fabjan, J. Power Sources 127 (2004) 98.
[4] M. Skyllas-Kazacos, F. Grossmith, J. Electrochem. Soc. 134 (1987) 2950.
[5] M.J. Watt-Smith, H. Al-Fetlawi, P. Ridley, R.G.A. Wills, A.A. Shah, F.C. Walsh, J. Chem. Technol. Biotechnol. 88 (2013) 126.
[6] S. Wang, X. Zhao, T. Cochell, A. Manthiram, J. Phys. Chem. Lett. 3 (2012) 2164.
[7] C. Flox, J. Rubio-García, M. Skoumal, T. Andreu, J.R. Morante, Carbon 60 (2013) 280.
[8] Y. Shao, X. Wang, M. Engelhard, C. Wang, S. Dai, J. Liu, Z. Yang, Y. Lin, J. Power Sources 195 (2010) 4375.
[9] B. Sun, M. Skyllas-Kazacos, Electrochim. Acta 37 (1992) 1253.
[10] D.J. Suárez, Z. González, C. Blanco, M. Granda, R. Menéndez, R. Santamaría, ChemSusChem 7 (2014) 914.
[11] B. Li, M. Gu, Z. Nie, X. Wei, C. Wang, V. Sprenkle, W. Wang, Nano Lett. 14 (2014) 158.
[12] K.J. Kim, M.-S. Park, J.-H. Kim, U. Hwang, N.J. Lee, G. Jeong, Y.-J. Kim, Chem. Commun. 48 (2012) 5455.
[13] D. Aaron, C.-N. Sun, M. Bright, A.B. Papandrew, M.M. Mench, T.A. Zawodzinski, ECS Electrochem. Lett. 2 (2013) A1.
[14] C.-N. Sun, F.M. Delnick, D.S. Aaron, A.B. Papandrew, M.M. Mench, T.A. Zawodzinski, ECS Electrochem. Lett. 2 (2013) A43.
[15] Q. Liu, A. Turhan, T.A. Zawodzinski, M.M. Mench, Chem. Commun. 49 (2013) 6292.
[16] C. Flox, M. Skoumal, J. Rubio-Garcia, T. Andreu, J.R. Morante, Appl. Energy 109 (2013) 344.
[17] D. You, H. Zhang, J. Chen, Electrochim. Acta 54 (2009) 6827.